Journal of Geoscience and Environment Protection, 2023, 11, 1-14
https://www.scirp.org/journal/gep
ISSN Online: 2327-4344
ISSN Print: 2327-4336

Regional Intrusive Signature from the Cameroon Coastal Basins to Bioko Island in Equatorial Guinea (Gulf of Guinea) Using Gravity Studies

Eric N. Ndikum[1,2*], Charles T. Tabod[3,4]

[1]Department of Physics, HTTC Bambili, The University of Bamenda, Bamenda, Cameroon
[2]Department of Fundamental Sciences, Higher Technical Teacher Training College (HTTTC), Bamenda, Cameroon
[3]Department of Physics, University of Yaoundé 1, Yaoundé, Cameroon
[4]Department of Physics, Faculty of Science, The University of Bamenda, Bamenda, Cameroon
Email: *ndikumeric@yahoo.com

How to cite this paper: Ndikum, E. N., & Tabod, C. T. (2023). Regional Intrusive Signature from the Cameroon Coastal Basins to Bioko Island in Equatorial Guinea (Gulf of Guinea) Using Gravity Studies. *Journal of Geoscience and Environment Protection, 11,* 1-14.
https://doi.org/10.4236/gep.2023.111001

Received: September 20, 2022
Accepted: January 10, 2023
Published: January 13, 2023

Abstract

The Gulf of Guinea constitutes an area of great petroleum potential yet with very limited geophysical research information. Consequently in this study, a Bouguer anomaly map has been computed from gravity data covering regions stretching from the Cameroon coastal basins to Bioko island (formerly Fernando Po) which is part of Equatorial Guinea. The data were further processed for Source Edge Detection (SED), Euler 3D deconvolution, 3D surface oriented models and 3D voxel solutions. The results confirmed the presence of previously identified intrusive bodies around the Douala and Kribi/Campo sedimentary sub-basins and went ahead to suggest a probable continuity between these two. A possible extension of this body offshore the Gulf of Guinea right up to Bioko island with very striking similarities was also highlighted and it shows characteristic variations in the depth to the surface of the body at different locations.

Keywords

Intrusive Body, 3D Surface-Oriented Model, Gulf of Guinea

1. Introduction

The Douala Sedimentary sub-basin and the Kribi-Campo Sedimentary sub-basin are all part of the Cameroon atlantic basin which stretch forth up to Bioko island (formerly Fernando Po) which is part of Equatorial Guinea (see **Figure 1**).

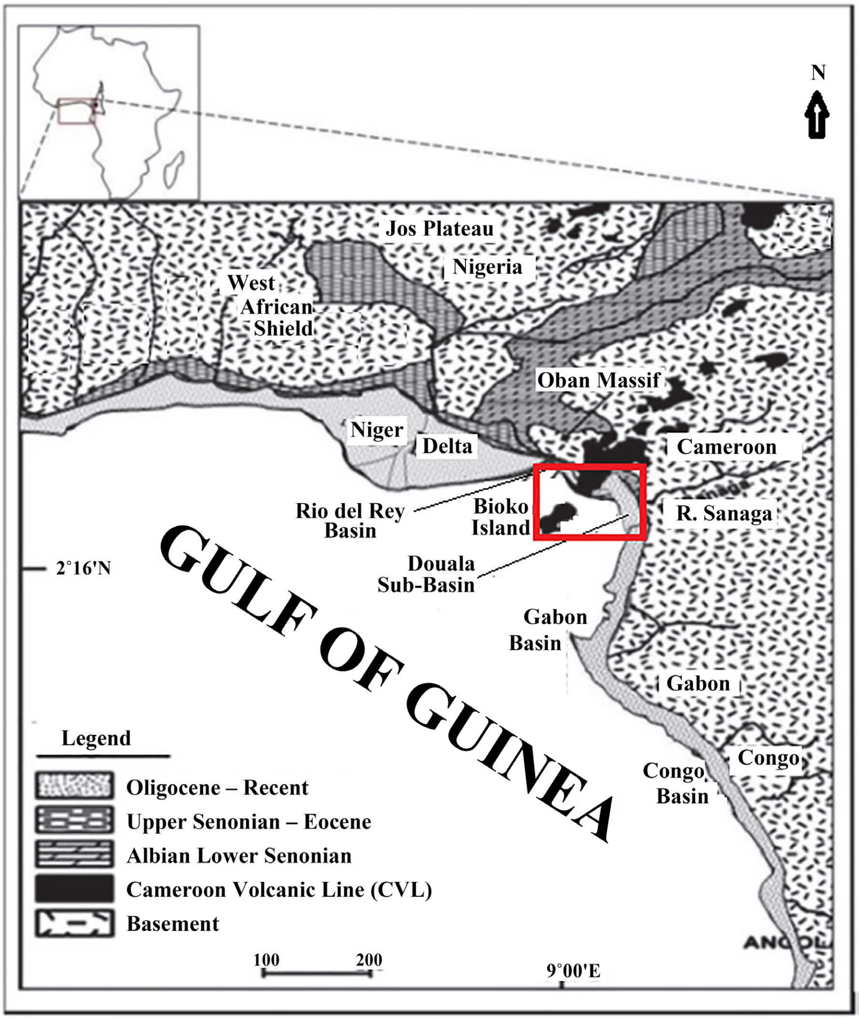

Figure 1. Map showing study area (as red rectangular box) modified after Anoh et al. (2018).

Cameroon and Equatorial Guinea in their coastal and offshore areas are part of the West-Central Coastal Province of the Sub-Saharan African Region (Brownfield & Charpentier, 2006). The Douala sedimentary sub-basin has an estimated depth ranging from about 6 to 7 km (Ala & Selley, 1997; Anoh et al., 2014, 2018).

Most of the geophysical/geological studies carried out in this region have been done by petroleum exploration firms and so their results are not published.

A number of geophysical studies have been carried out in different parts of this Coastal Province in recent times using different methods. Koumetio et al. (2009) carried out 2.5D gravity modelling along Bouguer gravity profiles to highlight two major structures in the southern part of the Douala sedimentary sub-basin. Ndikum et al. (2014, 2017) and Ndikum (2015) employed 2.5D studies along two profiles to establish the presence of an igneous intrusive body in the Douala sedimentary sub-basin of about 2.77 g/cm^3. Koumetio et al. (2012) suggested the presence of two dense intrusive igneous blocks in the upper crust in the Kribi-Edea zone whose surfaces lie locally at depths between 0.9 and 1 km, both having a density contrast of about 0.167 g/cm^3 in comparison to the surrounding metamorphic rocks. Further south of the Kribi-Campo sub-basin, to the SE edge around Bipindi, Koumetio et al. (2014) used 3D modelling techniques to characterize two dissymmetrical blocks of the same type of rock with density contrast of −0.095 g/cm^3. Malquaire et al. (2017) carried out 3D gravity modeling in the northern part of the Kribi-Campo sub-basin to indicate the presence of a dense intrusive igneous body of density 2.74 g/cm^3 in the upper crust. Ndikum et al. (2019a, 2019b) have also employed geophysical techniques of Euler 3Ddeconvolution, Source Edge Detection (SED), analysis of some special functions (horizontal gradient magnitude (HGM), analytic signal (AS) and the local wavenumber (LW)), 3D surface oriented models and 3D voxel solutions to characterise a 3D intrusive body and other structural lineaments in the Douala sub-basin.

Studies in different portions of both the Douala and Kribi-Campo sub-basins indicate the presence of intrusive materials with densities of approximately 2.7 g/cm^3. Bouguer maps of the Douala sub-basin are characterized by high positive anomalies which suggest the possibility of continuity beyond the South-West coastal portions. 3D surface oriented plots in the Douala sub-basin further emphasize this possible extension (Ndikum et al., 2019a). Consequently, the need arises to investigate on one hand if the intrusive bodies in the Douala & Kribi-Campo sub-basins are part of the same unit or separate entities. On the other hand, it is important to verify if these intrusive bodies continue beyond the Cameroon Atlantic basins and to what extent across the West-Central Coastal Province of the Sub-Saharan African Region.

2. Geologic and Tectonic Settings

The Douala/Kribi-Campo basin along with the Rio del Rey basin constitutes the Atlantic coastal basins of Cameroon. They are separated by a major tectonic feature, the Cameroon Volcanic Line. The two basins form part of a series of sedimentary fills lining the West African coast (Anoh et al., 2014). The Rio del Rey basin constitutes the eastern limb of the Benue trough and of the Niger Delta that infills it (Ala & Selley, 1997). The Mundeck formation crops out in the Rio del Rey basin as the oldest sediments in its onshore portion. It consists of coarse pebbly cross-bedded fluvial sandstones. Shallow marine limestones, sandstones and shales of the Mungo and Logbaba formations overlie these deposits. Offshore the Rio de Rey basin, a stratigraphic section which is broadly compared to the Niger Delta has been revealed by drilling (Short & Stauble, 1967). The Douala/Kribi-Campo basin is larger than the Rio del Rey basin and has a more continuous stratigraphic section. Its continental basal cretaceous sands are overlain by shallow marine limestones, sandstones and shales of Late cretaceous, Palaeogene and Neogene ages. Basaltic lavas from the Cameroon volcanic centre overlie these formations at the western margin of the basin (Ala & Selley, 1997).

Moving southwest from the Douala/Kribi-Campo basin offshore, is located Bioko island (formerly Fernando Po) which is part of Equatorial Guinea and constitutes part of the offshore portion of the Cameroon Volcanic Line (CVL) (Tokam et al., 2010). Further south, the Douala/Kribi-Campo basin is bounded by the Rio de Muni sedimentary basin which stretches over other portions of Equatorial Guinea. The Rio de Muni basin together with the Douala/Kribi-Campo basin constitutes a NNE-SSW orientated continental margin. They show a rift faulting that appears to have similar trends and is associated to a thick Aptian sedimentary section. Arcuate fault traces which broadly parallel the Rio de Muni coastline were later produced by post-rift gravity sliding (Lawrence et al., 2002).

The Tectonic evolution of the West African Coastal basins, which is similar to that of the Gulf of Guinea, is strongly related to the processes of rifting and drifting that resulted in the opening of the South Atlantic Ocean and which led to the separation of the South American plate from the African plate (Bate et al., 2019). This evolution was in three main stages, namely: Pre-rift (from Late Proterozoic to Late Jurassic), Syn-rift (from Late Jurassic to Early Creetaceous) and Post-rift (from Late Cretaceous to Holocene).

3. Data and Methodology

3.1. Data

A total of about 610 gravity data points were used in this study. This data was obtained from gravity surveys carried out by the Office de la Recherche Scientifiqueet Technique d'Outre-Mer (ORSTOM) (Collignon, 1968; Louis, 1970) which are made available by the Bureau Gravimétrique International (BGI, 2018)/IAG International Gravity Field Service. These data have average inter-station distances of 4 to 5 km. These data points were collected on the land leaving the marine section between the Cameroon Coastal basin and Bioko island without data points. A comparative analysis will be done with results obtained from the available data and results generated from the data complemented with dummy data points.

3.2. Methodology

3.2.1. Euler 3D Deconvolution

Euler 3D deconvolution method has been applied on Bouguer anomaly from the study area by means of the montaj Euler 3D deconvolution (Euler 3D) system to automatically determine the location and depth of the potential field in the region. The Standard Euler 3D method (Reid et al., 1990; Thompson, 1982) which is based on Euler's homogeneity equation and relates the potential field (gravity or magnetic) and its gradient components to the source location was used. This is done with a degree of homogeneity N, referred to as the structural index (Whitehead & Musselman, 2005).

Given a potential field $P(r, s, t)$, Euler's equation can be stated as:

$$(r-r_0)\frac{\mathrm{d}P}{\mathrm{d}r}+(s-s_0)\frac{\mathrm{d}P}{\mathrm{d}s}+(t-t_0)\frac{\mathrm{d}P}{\mathrm{d}t}=N(C-P) \quad (1)$$

With (r_0, s_0, t_0) the location of the potential field whose total field P is measured at (r, s, t) having a regional value of C while N is the Structural index (SI) whose values are presented in Table 1.

3.2.2. Source Edge Detection (SED)

This is a tool that is able to locate edges (geological contacts) or peaks from potential field data by analyzing the local gradients (Whitehead & Musselman, 2005). This is done by estimating the location of abrupt lateral changes in magnetization or mass density of rocks of the upper crust by identifying the maxima on a grid of horizontal gradient magnitudes. Localized peaks in gravity grids are identified using the Blakely and Simpson (1986) method and assigned one of the following levels:

"all 4 directions": grid values in all adjacent grid cells are lower

"3/4 directions": grid values in three directions are lower.

"2/4 directions": grid values in two directions are lower.

"1/4 direction": grid values in any one direction are lower (i.e. a ridge).

Plots of the source edges determined by SED are done for different peak levels with color-coded symbols (⊥). On these plots, the strike direction of the edge (contact) is represented by the direction of the long axis, while the "down-gradient" direction, pointing away from a locally and more dense or magnetized source, is shown by the dip indicator. When the results of SED are plotted on the Bouguer or residual anomaly map, the symbols indicate geological contacts or edges of geologic bodies.

3.2.3. 3D Surface Oriented Models

The Oasis Montaj tool, GM-SYS 3D (Geosoft Online Help, 2014), which uses calculations performed in the wave number (Parker, 1972), has been used to build depth models in order to provide surface-oriented models of the possible surface disposition of the intrusive body in this study area. These models are relief plots which indicate the variation in depth of surfaces with particular densities, where each surface is a constant layer at a specific density. A model with constant surface layer at 0 km and bottom layer at a depth of 40 km was generated. The geometry of the model was adopted from the residual field obtained at upward continuation height of 30 km (Ndikum et al., 2014; Ndikum, 2015).

Table 1. Structural index values for different gravity geologic models.

Geologic model	Number of infinite dimensions	Gravity SI
Sphere	0	2
Pipe	1 (z)	1
Horizontal cylinder	1 (x - y)	1
Dyke	2 (z and x - y)	0
Sill	2 (x and y)	0
Contact	3 (x, y and z)	undefined

The constant density value of 2.77 g/cm^3 suggested by the studies of Ndikum et al. (2014), Ndikum et al. (2017) and Koumetio et al. (2012) for the intrusive body in this region was used. The Bouguer data, used as the survey data, was loaded into the model with the background density of 2.5 g/cm^3 from the surrounding sedimentary basin (Telford et al., 1990). The calculated density contrast of the layer was determined through forward calculations while the density of the layer with respect to the forward calculations was recalculated using constant density inversion. From this point, the surface oriented model of the layer was generated through structural inversion.

3.2.4. 3D Voxel Solutions

Voxel is the short form of "volume pixel" which is used in three dimensional modeling and the discussion of data cubes; it actually signifies the smallest distinguishable box-shaped part of a three-dimensional image. This implies it is the 3D conceptual counterpart of the 2D pixel (Geosoft Online, 2014). Using the model from the surface oriented plot as the starting model, the geometry of the 3D voxel solution was defined. The 3D voxel solution for the intrusive body in this study area was then generated as well as the calculated anomaly map by employing the basic statistical kriging algorithm.

4. Results

4.1. Qualitative Analysis

The gravity data were gridded using the minimum curvature grid and displayed as a Bouguer map (**Figure 2**). The Bouguer anomaly is characterised by very high positive values which are concentrated towards the centre of the area of study. These high positive values are characteristic of the presence of intrusive material beneath the study area of the West-Central Coastal Province of the Gulf of Guinea. The high positive values generally stretch in a NE-SW direction from the NW portion of the Douala sub-basin right down to Equatorial Guinea. The anomaly is concentric in shape with a peak value of 105.1 mGal towards the SW of Limbe (longitude 9˚7'E and latitude 3˚58'N), a smaller peak with value 101.9 mGal further SW towards the SE of Malabo (longitude 8˚54'E and latitude 3˚38'N) and the greatest peak with value 126.3 mGal towards the E of Bioko (longitude 8˚40'E and latitude 3˚25'N). Towards the NE edge of the study area, a rapid change is noticed from positive to negative anomaly values which is suggestive of change in structure. This most probably marks the limit of the intrusive body. On the other sides of the peak portions, the anomalies are either continuous or decreasing steadily.

4.2. Euler 3D Deconvolution Solutions

Standard Euler 3D deconvolution was carried out on the Bouguer anomaly in the study area for structural index value of 0 in order to estimate the depth of the different geologic bodies responsible for this anomaly. The results (**Figure 3(a)**) suggested that majority of the bodies were located at depths of about 4 to 5 km.

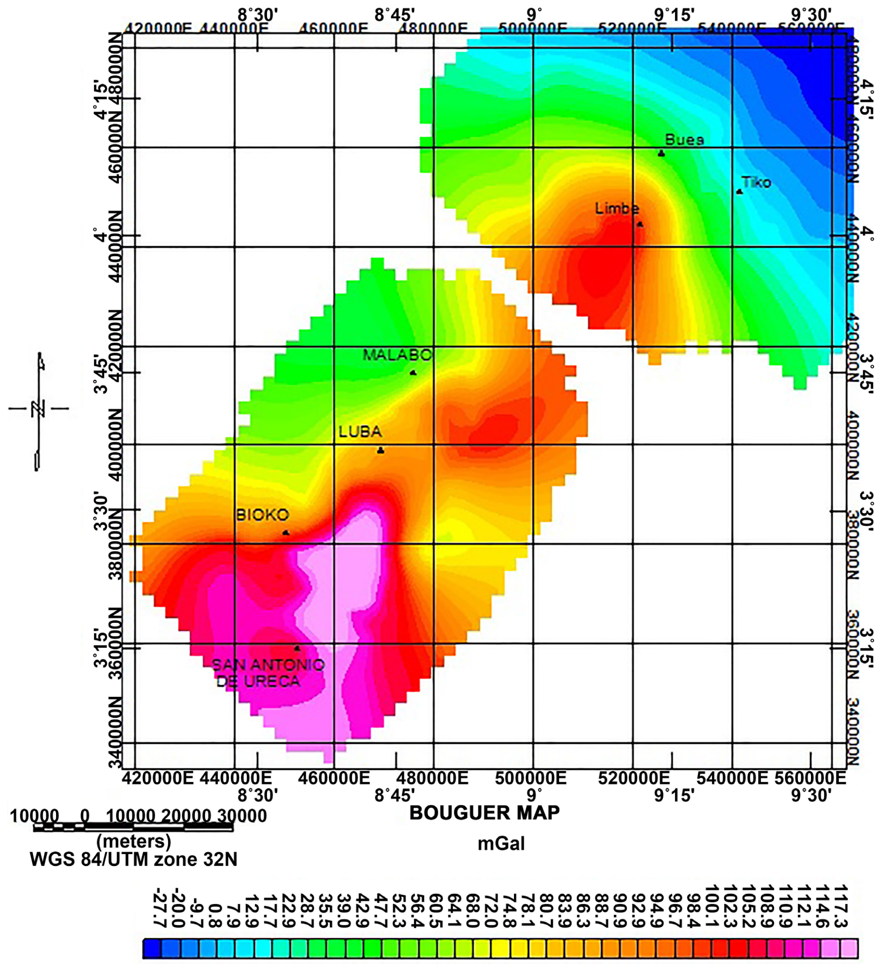

Figure 2. Bouguer map of the study area.

Some peaks however are noticed to be located closer to the surface at depths of about 2 km. These contacts were most pronounced along the NE edge of the study area where there is an abrupt change in anomaly and also towards the NW limit of the positive high portion. For Euler 3D analysis on the Bouguer anomaly data augmented with dummies (**Figure 3(b)**), these limits are further emphasized as well as indications of peak positions in the study area. This suggests that, with the availability of data points on unrepresented areas, a better picture will be obtained which will justify the continuity of the body in this study area. Worth noting is the fact that, the number of depth locations are most likely few in number as a result of the broadness of the surface area over which the analysis have been carried out.

4.3. Solutions of Source Edge Detection

The Source Edge Detection (SED) method was applied on the Bouguer anomaly and results for peak values ranging from 2 to 4 plotted on the Bouguer anomaly map (**Figure 4(a)**). The plots indicate generally that the dip directions of all peak values are pointing away from the positive high region on the Bouguer anomaly

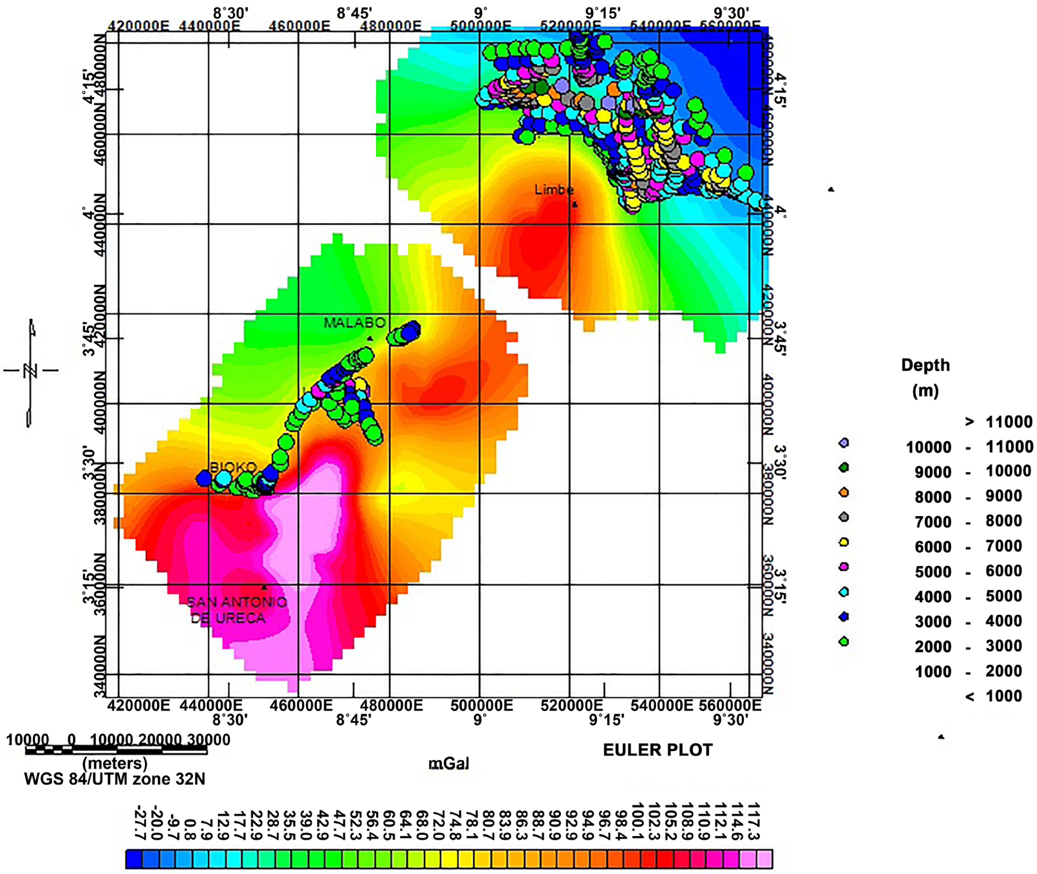

(a)

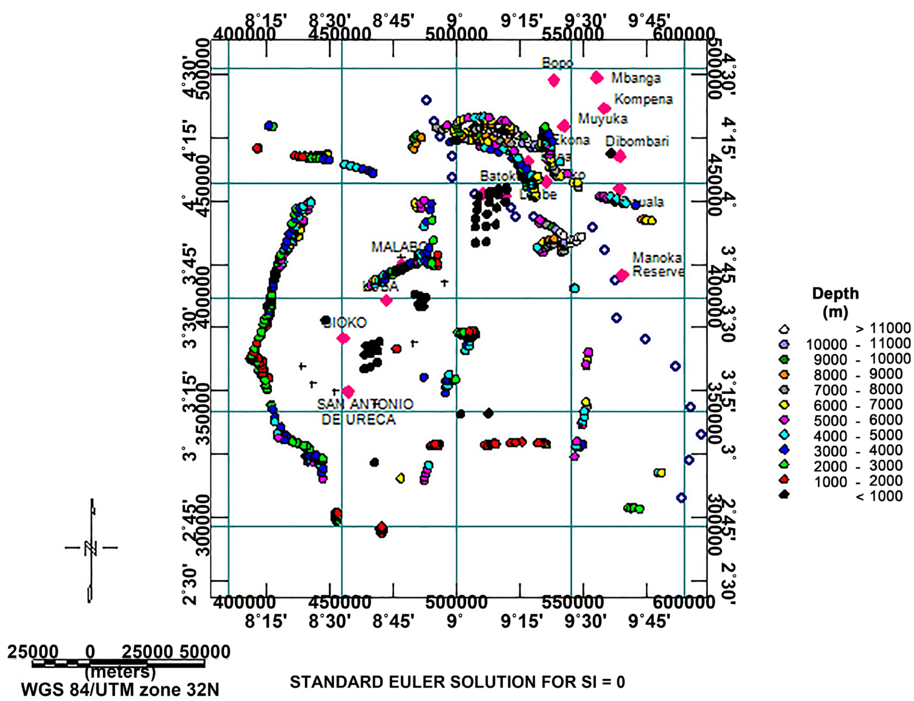

(b)

Figure 3. (a) Plot of Euler 3D deconvolution results; (b) Plot of Euler 3D deconvolution results with dummy values included.

map. It can also be observed that this is especially the case around the positions of the three major peaks on this map. The outline of the possible edges of the structures in this study area is further emphasized when the SED is carried out and plotted for Bouguer anomaly augmented with dummy values (**Figure 4(b)**). This plot goes ahead to establish the continuity of the edges of the structures beneath this study area across the area with limited data.

4.4. 3D Surface Oriented Model Solutions

The plot of the 3D surface oriented model (**Figure 5**) obtained using GM-SYS 3D presents a body with a calculated density of about 2.769 g/cm^3 from an initial constant layer located at a depth of about 33 km. This model constitutes a surface which is continuous across the entire study area with varying depths to its peak at different points in the study area. The surface is seen to continue towards the South in the direction of the Kribi-Campo sub basin and further South West right up to Bioko island with a link beneath the offshore section. The high positive anomaly which was noticed beneath the Douala sub-basin is shown to correspond to major peak of the intrusive body at a depth of about 5 km. The high

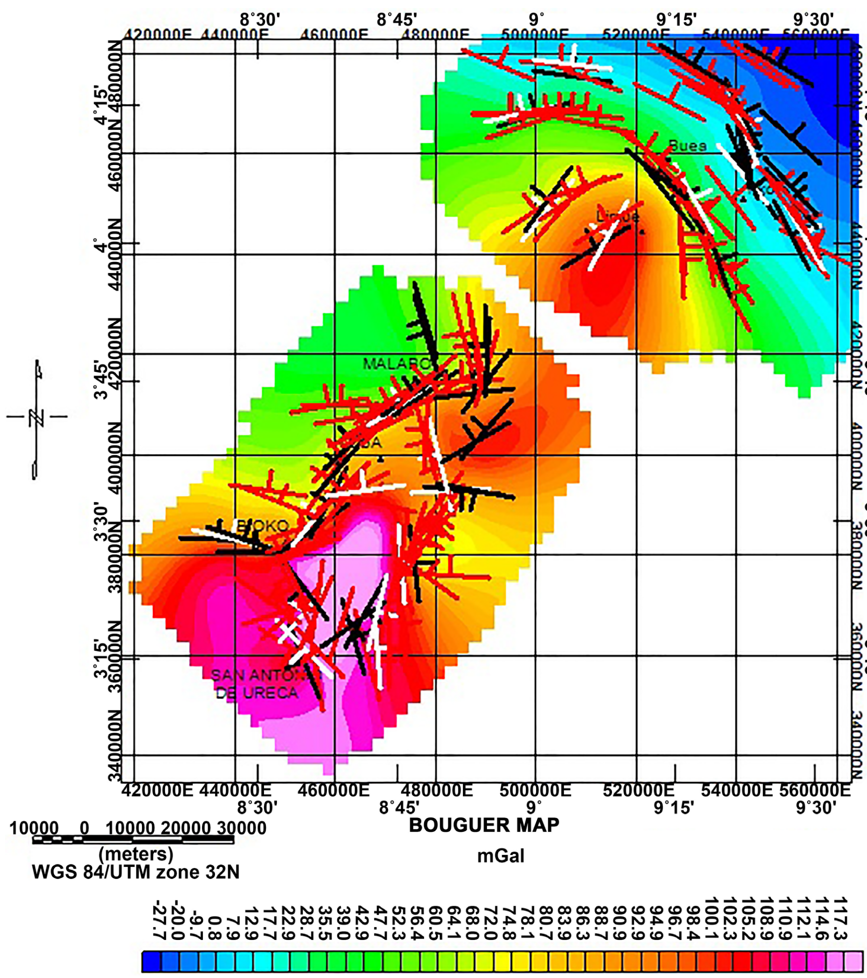

(a)

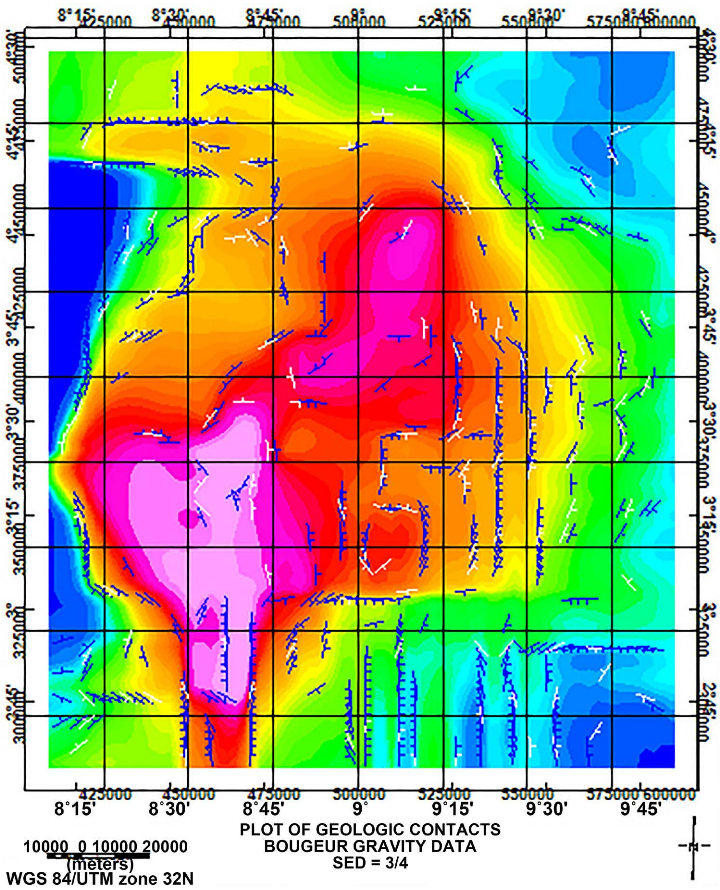

(b)

Figure 4. (a) Plot of source edge detection solutions. The peak colour-coded symbol (⊥) is red for peak value 2, black for peak value 3 and white for peak value 4. (b) Plot of Source Edge Detection solutions with dummy values included.

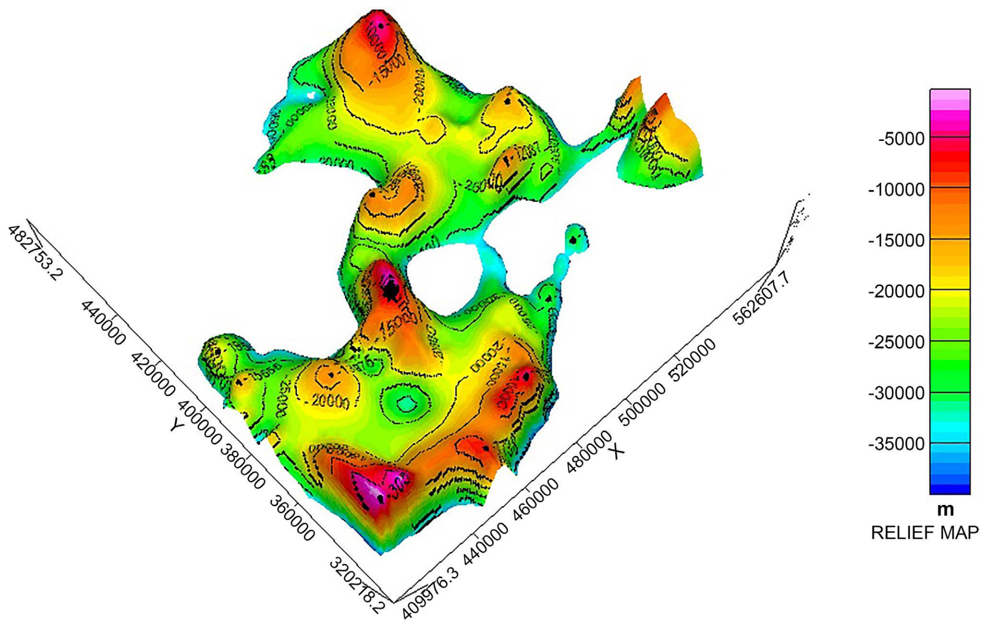

Figure 5. Plot of surface oriented model.

positive anomaly beneath Bioko island also corresponds to the peak of the intrusive body at a depth of about 2.6 km. This smaller depth value explains why the Bouguer anomaly had a higher value around Bioko island than around the Douala sub-basin.

4.5. 3D Voxel Solution

The 3D surface oriented model was then used to generate the 3D voxel solution (**Figure 6**) of the block structure underlying this surface using GM-SYS 3D. The

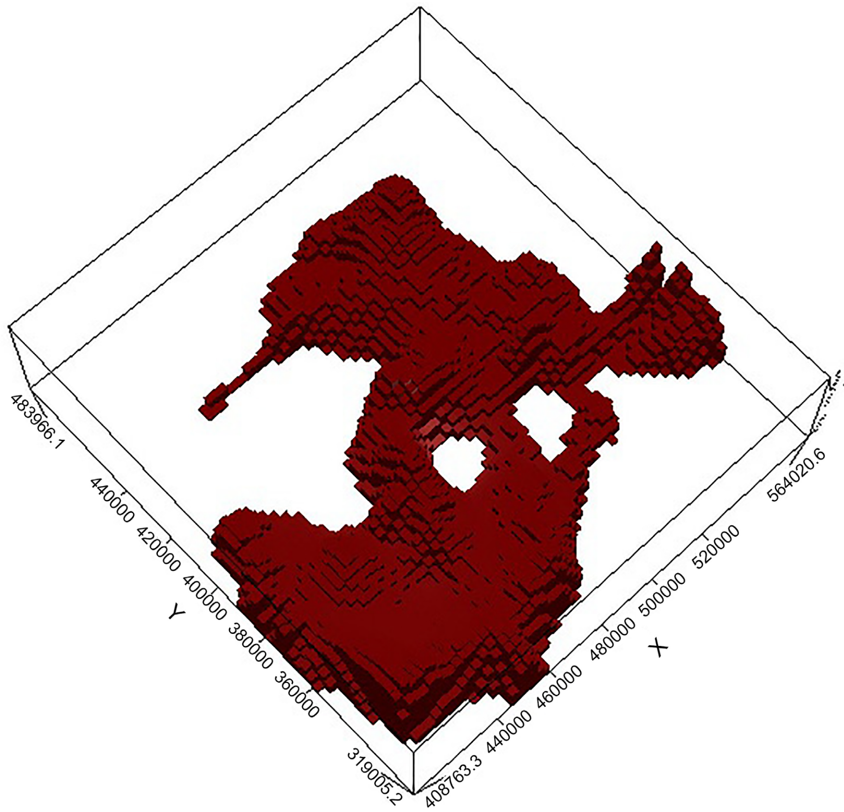

Figure 6. Plot of 3D Voxel solution.

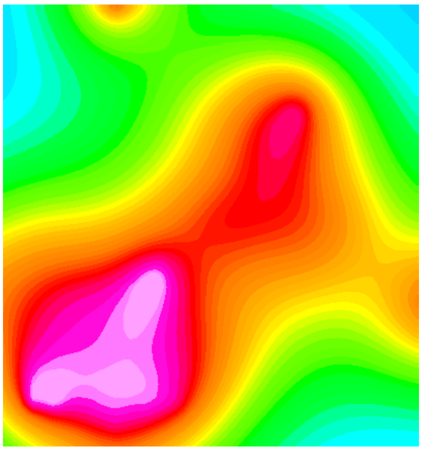

Figure 7. Plot of calculated anomaly from model.

3D voxel solution presented a block structure corresponding to an intrusive body of density 2.77 g/cm^3 underlying the surface generated by the 3D surface oriented model. This block structure still indicated that the intrusive body continued towards the Kribi-Campo sub basin and also extended right up to Bioko island. The calculated anomaly map (**Figure 7**) from this 3D voxel solution showed very striking similarities with the Bouguer anomaly map (**Figure 2**) of the study area as far as the high positive anomaly values and the peak positions are concerned.

5. Conclusion

Gravity data covering a surface area stretching from the Douala/Kribi-Campo sedimentary basin to and including Bioko island in Equatorial Guinea has been processed to plot the Bouguer anomaly map. The high positive values of the Bouguer anomaly stretching in the NE-SW direction and constituted by circular-like contours were seen to be indicative of an intrusive body. Euler 3D deconvolution analysis located the depth to the causative geologic body to a minimum depth of about 2 km but also suggested that majority of the bodies were located between a depth range of 4 to 5 km. Source edge detection analysis traced possible edges of this body with dip directions generally pointing outwards from the center of the peak anomaly region which is characteristic of intrusion. 3D surface oriented modelling as well as 3D voxel solution generated from the Bouguer data both presented an intrusive body which extends southwards into the Kribi-Campo sub basin and also towards the south west right up to Bioko island in Equatorial Guinea. This model was observed to be of igneous origin with density of about 2.769 g/cm^{3}and depths of about 2.6 km and 5 km beneath the Bioko island and Douala sub basin respectively.

Acknowledgements

The authors are grateful to the Bureau Gravimétrique International (BGI) for making available the gravity data that has been used to carry out this study. Their appreciation also goes to the anonymous reviewers of this paper.

Conflicts of Interest

The authors declare no conflicts of interest regarding the publication of this paper.

References

Ala, M. A., & Selley, R. C. (1997). Chapter 8. The West African Coastal Basins. *Sedimentary Basins of the World, 3,* 173-186. https://doi.org/10.1016/S1874-5997(97)80011-1

Anoh, N. O., Ama, E. J., & Atud, T. (2014). Abian-Turonian Palynomorphs from the Mundeck and Logbadjeck Formations, Ediki River, North-Western Part of the Douala Sub-Basin, Cameroon. *Sciences, Technologies et Developpement, 15,* 66-77.

Anoh, N. O., Njoke, M. L., & Elangwe, N. D. (2018). Cretaceous-Tertiary Foraminifera and Palynomorphs from Djega Section and Inferred Paleodepositional Environments, Rio Del Rey Basin, Cameroon, West Africa. *The Scientific World Journal, 2018,* Article ID: 6126528. https://doi.org/10.1155/2018/6126528

Bate, B. B., Ozumba, M. B., Ndip, E. A., & Eyinla, D. S. (2019). A Review of the Geology of the Rio Del Rey Basin, Offshore Cameroon. *Journal of Petroleum & Environmental Biotechnology, 10,* 389. https://doi.org/10.35248/2157-7463.19.10.389

Blakely, R. J., & Simpson, R. W. (1986). Approximating Edges of Source Bodies from Magnetic or Gravity Anomalies. *Geophysics, 51,* 1494-1498. https://doi.org/10.1190/1.1442197

Brownfield, M. E., & Charpentier, R. R. (2006). *Geology and Total Petroleum Systems of the West-Central CoastalProvince (7203), West Africa*. US Geological Survey Bulletin 2207-B. http://www.usgs.gov/bul/2207/B

Bureau Gravimétrique International (BGI), Gravity Data Downloaded on July 19, 2018. https://bgi.obs-mip.fr

Collignon, F. (1968). *Gravimetrieet Reconnaissance de la RepubliqueFederale du Cameroun. [Gravimetry and Recognition of the Federal Republic of Cameroon]* (Vol. 35). ORSTOM.

Geosoft Online Help @ 2014 Geosoft Inc. https://www.geosoft.com

Koumetio, F., Tabod, C. T., & Manguelle-Dicoum, E. (2009). Evidence for Upper Mantle Intrusion in the West African Coastal Sedimentary Basins from Gravity Data: The Case of the Southern Part of the Douala Basin, Cameroon. *Global Journal of Geological Sciences, 7,* 181-187. https://doi.org/10.4314/gjgs.v7i2.51606

Koumetio, F., Njomo, D., Tabod, C. T., Noutchogwe, T. C., & Manguelle-Dicoum, E. (2012). Structural Interpretation of Gravity Anomalies from the Kribi-Edea Zone, South Cameroon: A Case Study. *Journal of Geophysics and Engineering, 9,* 664-673. https://doi.org/10.1088/1742-2132/9/6/664

Koumetio, F., Njomo, D., Tatchum, C. N., Tokam, K. A. P., Tabod, C. T., & Manguelle-Dicoum, E. (2014). Interpretation of Gravity Anomalies by Multi-Scale Evaluation of Maxima of Gradients and 3D Modelling in Bipindi Region (South-West Cameroon). *International Journal of Geosciences, 5,* 1415-1425. https://doi.org/10.4236/ijg.2014.512115

Lawrence, S. R., Munday, S., & Bray, R. (2002). Regional Geology and Geophysics of the Eastern Gulf of Guinea (Niger Delta to Rio Muni). *The Leading Edge, 21,* 1112-1117. https://doi.org/10.1190/1.1523752

Louis, P. (1970). *Contribution Geophysiquea la Connaissance Geologique du Bassin du lac Chad*. ORSTOM.

Malquaire, K. P. R., Louise, O. A. M., Nfor, N., & Eliezer, M.-D. (2017). 3D Modelling from New and Existing Gravity Data of an Intrusive Body in the Northern Part of Kribi-Campo Sub-Basin in Cameroon. *International Journal of Geosciences, 8,* 984-1003. https://doi.org/10.4236/ijg.2017.88056

Ndikum, E. N. (2015). *Gravity Study of the Douala Sedimentary Basin* (pp. 1-91). PhD Thesis, Dept. of Physics, Faculty of Science, University of Yaounde I.

Ndikum, E. N., Kenfack, J. V., Koumetio, F. et al. (2019a). Voxel Solution and 3D Sub-Surface Imaging in the Douala Sedimentary Sub-Basin (Cameroon). *Physics of the Earth and Planetary Interiors, 294,* Article ID: 106293. https://doi.org/10.1016/j.pepi.2019.106293

Ndikum, E. N., Koumetio, F., Victor Kenfack, J., & Tabod, C. T. (2019b). Gravity Study of the Douala Sub-Basin (Cameroon) Using Euler 3D Deconvolution, Source Edge Detection (SED) and Special Function Analysis. *SN Applied Sciences, 1,* Article No. 1200. https://doi.org/10.1007/s42452-019-1176-y

Ndikum, E. N., Tabod, C. T., Essimbi, B. Z., Koumetio, F., & Noutchogwe, C. T. (2014). Gravity Model for an Anomalous Body Located in the NW Protion of the Douala Sedimentary Sub-Basin, Cameroon (Central Africa). *Open Journal of Geology, 4,* 524-541. https://doi.org/10.4236/ojg.2014.410039

Ndikum, E. N., Tabod, C. T., Koumetio, F., Tatchum, N. C., & Victor, K. J. (2017). Evidence of Some Major Structures Underlying the Douala Sedimentary Sub-Basin: West African Coastal Basin. *Journal of Geoscience and Environment Protection, 5,* 161-172. https://doi.org/10.4236/gep.2017.57013

Parker, R. L. (1972). The Rapid Calculation of Potential Anomalies. *Geophysical Journal of the Royal Astronomical Society, 31,* 447-455. https://doi.org/10.1111/j.1365-246X.1973.tb06513.x

Reid, A. B., Allsop, J. M., Granser, H. et al. (1990). Magnetic Interpretation in Three Dimensions Using Euler Deconvolution. *Geophysics, 55,* 80-91. https://doi.org/10.1190/1.1442774

Short, K. C., & Stauble, A. J. (1967). Outline of Geology of Niger Delta. *AAPG Bulletin, 51,* 761-779. https://doi.org/10.1306/5D25C0CF-16C1-11D7-8645000102C1865D

Telford, W. M., Geldart, L. P., & Sheriff, R. E. (1990). *Applied Geophysics* (2nd ed., pp. 6-61). Cambridge University Press. https://doi.org/10.1017/CBO9781139167932

Thompson, D. T. (1982). EULDPH: A New Technique for Making Computer-Assisted Depth Estimates from Magnetic Data. *Geophysics, 47,* 31-37. https://doi.org/10.1190/1.1441278

Tokam, K. A. P., Tabod, C. T., Nyblade, A. A., Julia, J., Wiens, D. A., & Pasyanos, M. (2010). Structure of the Crust Beneath Cameroon, West Africa, from the Join Inversion of Rayleigh Wave Group Velocities and Receiver Functions. *Geophysical Journal International, 183,* 1061-1076. https://doi.org/10.1111/j.1365-246X.2010.04776.x

Whitehead, N., & Musselman, C. (2005). *MontajGrav/Mag Interpretation, Tutorial and User Guide* (pp. 1-77). Geosoft Inc. https://www.geosoft.com